Deep-Sea Research I 67 (2012) 21–31

Contents lists available at SciVerse ScienceDirect

Deep-Sea Research I

journal homepage: www.elsevier.com/locate/dsri

Spatial heterogeneity and underlying geochemistry of phylogenetically diverse orange and white *Beggiatoa* mats in Guaymas Basin hydrothermal sediments

Luke J. McKay [a], Barbara J. MacGregor [a], Jennifer F. Biddle [a,1], Daniel B. Albert [a], Howard P. Mendlovitz [a], Daniel R. Hoer [a], Julius S. Lipp [b], Karen G. Lloyd [a,2], Andreas P. Teske [a,*]

[a] Department of Marine Sciences, University of North Carolina at Chapel Hill, Chapel Hill, NC 27599, USA
[b] Organic Geochemistry Group, MARUM Center for Marine Environmental Sciences and Department of Geosciences, University of Bremen, Bremen, D-28334, Germany

ARTICLE INFO

Article history:
Received 15 December 2011
Received in revised form
23 April 2012
Accepted 25 April 2012
Available online 5 May 2012

Keywords:
Beggiatoa
Guyamas Basin
Hydrothermal vents
Microbial mats

ABSTRACT

Sulfide-oxidizing bacteria of the genus *Beggiatoa* are found in conspicuous, colorful mats on the seafloor above active hydrothermal seeps at Guaymas Basin. Guaymas *Beggiatoa* filaments fall into discrete size classes representing at least five separate 16S rRNA phylotypes, and appear either white, yellow, or orange. During two R/V *Atlantis* cruises to Guaymas Basin, 78 temperature profiles were taken near and within 15 different orange and white *Beggiatoa* mats by the *Alvin* submersible to investigate spatial relationships between mat color and hydrothermal fluid seeps, as indicated by elevated temperatures. The surface temperatures from 78 profiles are similar to each other (on average 8–12 °C, warmer than bare sediments at 3–4 °C), indicating that Guaymas Basin *Beggiatoa* spp., although relying on the hydrothermal system for energy and carbon sources, live within a relatively cool temperature range. Temperatures from 40 cm below orange *Beggiatoa* versus white *Beggiatoa* are the same, at 84 °C averaged across all mat systems. However, within a single mat system, temperatures are higher beneath the predominantly orange center of the mat than beneath the white mat periphery. Push core transects across the orange-to-white color change of three *Beggiatoa* mats showed stronger upward compression of isotherms and metabolic zones beneath the orange mat center than beneath white mat periphery. Hydrothermal temperature gradients push the microbial processes generating carbon and energy sources for *Beggiatoa* mats towards the sediment surface. The resulting steep gradients of hydrothermal electron donors and carbon sources to the sediment surface, rather than the in situ temperature by itself, control the relative positioning of orange and white filaments within a Guaymas Basin *Beggiatoa* mat. Given the wide spectrum of temperature and hydrothermal flux regimes between different mats, the orange/white pattern represents a relative preference or even a competitive balance among different *Beggiatoa* types that establishes itself within each hydrothermal hot spot.

1. Introduction

Seafloor spreading centers are associated with hydrothermal activity and are typically found in open ocean regions with very low sedimentation rates. The Guaymas Basin in the Gulf of California is a unique, relatively near-shore spreading center characterized by hydrothermal fluids that rise through a 300–400 m layer of pelagic and terrigenous organic-rich sediments before escaping at the seafloor (Einsele et al., 1980). Hydrothermal fluids that seep through the thick sediment layer have temperatures greater than 300 °C at depth (Edmond and Von Damm, 1985; Van Damm et al., 1985). The upward transport of methane, organic acids, hydrogen, carbon dioxide, ammonia, and hydrogen sulfide in hydrothermal flow supplies metabolic substrates to a highly diverse microbial community carrying out metabolic processes such as methanogenesis, methane oxidation, nitrification, sulfate reduction, and sulfide oxidation (Dhillon et al., 2003, 2005; Teske et al., 2002, 2009).

Beggiatoa spp. are mat-forming, filamentous, sulfide-oxidizing bacteria that colonize the surface of sulfide-rich sediments. With filament and cell diameters of up to 200 μm, they are among the largest prokaryotes (Schulz and Jørgensen, 2001). At Guaymas Basin, *Beggiatoa* filaments range from only a few μm to more than 100 μm in diameter (Jannasch et al., 1989; Nelson et al., 1989).

* Corresponding author. Tel.: +1 919 843 2463.
E-mail address: teske@email.unc.edu (A.P. Teske).
[1] Present address: *School of Marine Science & Policy, University of Delaware Lewes, DE 19958, USA.*
[2] Present address: *Department of Microbiology, University of Tennessee-Knoxville, Knoxville, TN 37996, USA.*

0967-0637/$ - see front matter © 2012 Elsevier Ltd. All rights reserved.
http://dx.doi.org/10.1016/j.dsr.2012.04.011

The intracellular volume of Guaymas *Beggiatoa* cells is taken up almost entirely by a large vacuole, while the cytoplasm is only a thin layer between the vacuole and cell membrane (Jannasch et al., 1989; Nelson et al., 1989). In most cases, these large vacuoles accumulate and store nitrate (McHatton et al., 1996), although exceptions are known (Kalanetra et al., 2004). The thin periplasmic space sometimes contains globules of elemental sulfur, and these, along with stored nitrate in the vacuoles, likely sustain filaments during periods of inadequate electron donor or acceptor supply (Strohl et al., 1982; Jannasch et al., 1989; McHatton et al., 1996). In strong contrast to the brown sediments of Guaymas Basin, *Beggiatoa* spp. form conspicuous white, yellow, and orange mats around sites of active hydrothermal venting (Jannasch et al., 1989; Gundersen et al., 1992). The orange pigmentation in *Beggiatoa* filaments is attributed to high cytochrome content (Prince et al., 1988) based on examination of *Beggiatoa* mat sample 1615B, a suspension of brightly colored filaments of a single width class with filament diameters of mostly 25 to 35 μm (Nelson et al., 1989). The predominant cytochrome in at least one orange Guaymas *Beggiatoa* mat has recently been identified as an octaheme cytochrome with homology to hydroxylamine and hydrazine oxidoreductases (MacGregor et al., 2012). The white coloration is due to the refractive nature of elemental sulfur granules stored in the periplasm (Schulz and Jørgensen, 2001). It is currently unclear whether the source of the yellow coloration in *Beggiatoa* mats is intracellular or extracellular. The colorful *Beggiatoa* mats at the surface of otherwise brown sediments are visual markers for complex subsurface microbial communities taking advantage of the electron donor and carbon supply in hydrothermal vents and hydrocarbon seeps (Lloyd et al., 2010). *Beggiatoa* mats with both white and orange filaments show a consistent pattern: orange *Beggiatoa* spp. appear more concentrated than white filaments in the center of the mat, whereas only white filaments occur at the mat periphery. This spatial heterogeneity of *Beggiatoa* filament colors is seen on hot Guaymas Basin sediments and cold Gulf of Mexico sediments (Wirsen et al., 1992; Sassen et al., 1994; Larkin and Henk, 1996; Nikolaus et al., 2003), and suggests different habitat preferences of these *Beggiatoa* types. During two R/V *Atlantis* cruises to Guaymas Basin (December 5–17, 2008; November 22 to December 6, 2009), the association of *Beggiatoa* mats with hydrothermal seepage and the habitat preferences of various *Beggiatoa* types were investigated by geochemical and microbiological characterization of sediments underneath *Beggiatoa* mats in combination with temperature measurements down to 40 cm sediment depth. In particular, temperature profiles and corresponding sulfide, sulfate, dissolved inorganic carbon (DIC), δ^{13}C-DIC, methane, and δ^{13}C-methane gradients from mats exhibiting orange-to-white color transitions were examined to elucidate hydrothermal fluid delivery and/or tolerance associated with differently colored *Beggiatoa* types.

2. Materials and methods

2.1. Isolation of single Beggiatoa filaments, 16S rRNA gene amplification, and phylogenetic identification

On board the R/V *Atlantis* in 1998, *Beggiatoa* filaments collected either by push coring or "slurp gun" from the *Alvin* submersible were selected as single filaments with a pipette and dragged through soft agar (agarose and sterile seawater, 1:1) for about a minute before being stored at −80 °C in 50 μl centrifuge tubes. The orange and white *Beggiatoa* filaments collected in the 1998 cruise were amplified by polymerase chain reaction (PCR) as described previously, without prior whole-genome amplification (Teske et al., 1999). In 2008 and 2009, *Beggiatoa* spp. collected either by push coring or "slurp gun" from the *Alvin* submersible were first diluted into sterile seawater and subsequently diluted into a sterile 0.1% agar in seawater solution. Filaments were then visualized at 40X in a dissection microscope to assess size and color (Table S1, supplemental information). Single filaments were collected by pipetting with a 10 μl pipette tip. Filaments, along with 2–3 μl of sterile fluid, were placed into sterile PCR tubes and frozen at −80 °C. Samples were then transported to the laboratory at UNC-Chapel Hill for further analysis. In Chapel Hill, single filaments were centrifuged briefly and 10 μl of sterile water was added to each tube. After pipetting up and down vigorously to homogenize the filament–water mixture, 5 μl was used for full genome amplification according to the recommended protocol in the Qiagen Ultra-fast miniprep kit (Qiagen, Germantown, MD). From the amplified genome, the gene sequence for the 16S ribosomal RNA was amplified by PCR using the B8F bacterial forward primer (AGR GTT TGA TCC TGG CTC AG) and the B1492R bacterial reverse primer (CGG CTA CCT TGT TAC GAC TT) (Teske et al., 2002). PCR amplifications were run in BioRad iCycler Thermal Cycler (Hercules, CA). Each PCR reaction consisted of 2 μl amplified *Beggiatoa* genome, 2.5 μl 10X FBI buffer (TaKaRa, Shiga, Japan), 2.0 μl dNTP mix, 2.0 μl 10 μM B8F (Invitrogen, Carlsbad, CA), 2.0 μl 10 μM B1492R (Invitrogen), and 0.25 μl SpeedStar Taq polymerase (TaKaRa), and was brought to 25 μl with sterile H_2O. A preliminary melting period of 2 min at 94 °C was followed by 30 cycles of the following steps: 10 s at 98 °C, 15 s at 58 °C, and 20 s at 72 °C. These cycles were followed by 5 min at 72 °C and the final temperature was brought down to 12 °C. Amplifications were confirmed by gel electrophoresis followed by staining with ethidium bromide and visualization under ultraviolet light. Amplicons were cloned using the TOPO TA cloning kit (Invitrogen) and 3–5 individual colonies per filament were sent to GeneWiz (South Plainfield, NJ) for sequencing.

Near-complete 16S rRNA gene sequences were analyzed using Sequencher (Gene Codes, Ann Arbor, MI) and confirmed as closely related (95% maximum identity) to other non-Guaymas *Beggiatoa* spp. via the Basic Local Alignment Search Tool (BLAST) of the National Center for Biotechnology Information (http://blast.ncbi.nlm.nih.gov/). Next, the sequences were incorporated into a 16S rRNA alignment with sequences from related Gammaproteobacteria using the ARB phylogeny software package (Ludwig et al., 2004) and the SILVA v95 database (Pruesse et al., 2007). A phylogenetic tree was constructed using ARB's neighbor-joining function with Jukes–Cantor correction. Sequences were deposited at NCBI Genbank with accession numbers JN793553 through JN793557 (Table S1, supplemental information).

2.2. Temperature profiling

During *Alvin* dives 4483–4492 (Dec 6–17, 2008) and 4562–4573 (Nov 22–Dec 6, 2009) in the 2000 m deep Southern Guaymas trench, 113 temperature profiles were taken in sediments near and within *Beggiatoa* mats, at the hydrothermally active areas from 27°N00.30 to 27°N00.60, and 111°W24.65 to 111°W24.35 (Table S2, supplemental information). All temperature probe measurements, positions of the probe in the mat, and penetration depths were checked with the *Alvin* dive videotapes that provide a continuous record of all dive operations. Of the 113 temperature profiles, 78 were measured in mats with both orange and white filaments to focus on the relationship between differently colored *Beggiatoa*. A Heatflow probe manufactured by the Woods Hole Oceanographic Institution (WHOI) was used to measure 69 of the 78 temperature profiles. This is a 0.6 m titanium tube containing a linear heater and five thermistors (type 44032, Omega Engineering, Inc.) at 10 cm intervals along the length of the tube (personal communication with Lane J. Abrams, WHOI).

The thermistors have a tolerance of +/−0.2 up to 40 °C, and +/−1 °C up to 200 °C. It is considered fully inserted when a disk at the base reaches the sediment surface, and takes temperature readings at 0, 10, 20, 30 and 40 cmbsf. For 28 profiles, 5 cm depth resolution was achieved by first inserting the probe 5 cm less than complete insertion and recording one profile, and then inserting the probe the rest of the way and recording a second profile, 5 cm offset from the first. Temperatures were recorded after the readings had stabilized for each of the five depths. Occasionally, this technique resulted in channel formation, and the second set of readings was higher than the first. During dive 4490, one temperature profile was repeated three times, giving a range of sensor precisions from 1.0 to 4.1 °C. A high temperature probe was used to produce nine additional temperature profiles with varying depth intervals from the sediment surface down to 37.5 cmbsf. The high temperature probe has a type-K thermocouple located at the tip, with a tolerance of +/−3 °C up to 400 °C. To measure temperature profiles with this probe, the tip touched the sediment surface for the first reading before inserting the probe sequentially to desired depths and taking readings.

2.3. Statistical analysis

To analyze the relationship of sediment depth and mat color to surface and subsurface temperatures we performed a 2-way analysis of variance (ANOVA) using SigmaStat (Systat Software, San Jose, CA). Because data violated both normality and equal variance, α (2) values were reduced so that $p < 0.005$. *Post-hoc* Tukey tests were performed to estimate differences between treatment levels and the results were plotted using SigmaPlot (Systat Software, San Jose, CA). The clearest images of *Beggiatoa* mats captured by the submersible's high definition cameras were used to create maps indicating all temperature measurement locations in relation to mat cover with Adobe Photoshop CS (Adobe Systems, San Jose, CA). Two red lasers that project from *Alvin* 10 cm apart were used to create scale bars.

2.4. Three-dimensional reconstruction of temperature field

A three-dimensional reconstruction of the temperature field below "MegaMat" (27°N0.459, 111°W24.526), the largest mat observed during the 2008 cruise, was performed based on 14 temperature profiles that were systematically collected for this location on Dive 4485 (Dec 8, 2009). Linear interpolation of measured temperature profiles between 0 cm and maximum measured depth was performed in 5 cm resolution with MatLab (The MathWorks, Natick, MA). Final temperature grids were calculated for each depth horizon using the triangle interpolation scheme of the MatLab function "gridfit" (MatLab Central, http://www.mathworks.com/matlabcentral/fileexchange/). Shorter temperature profiles that did not reach 40 cm down were not extrapolated; in such cases only data within the measured depth interval was used for calculation of the temperature grids.

2.5. Porewater geochemistry

For porewater analyses, 50 ml Falcon tubes were filled completely with sediment; the sediment samples were centrifuged and the resulting porewater was immediately filtered using 0.45 μm syringe filters. For sulfate measurements, a 1 ml subsample was acidified with 50 μl of 50% HCl and bubbled with nitrogen for 4 min to remove sulfide. Sulfate was analyzed aboard the ship using a 2010i Dionex ion chromatograph (Sunnyvale, CA), as previously described (Martens et al., 1999). A separate 1 ml porewater subsample was drawn into a syringe containing 0.1 ml of 0.1 M zinc acetate solution to preserve the sulfide as zinc sulfide until analyzed. Sulfide was analyzed spectrophotometrically aboard the ship using the method reported by Cline (1969). For DIC, 2–3 ml of porewater were added to an evacuated 30 ml vial, stored upside down at −20 °C, and transported back to the lab at UNC for GC/C/IRMS analysis. For methane, prior to centrifugation 5.0 ml of sediment were added to 2.0 ml of 1 M NaOH in a 30 ml serum vial, mixed, and stored at −20 °C until GC/C/IRMS analysis at UNC. Concentrations and stable isotopic compositions of methane and DIC were measured using a Hewlett Packard 5890 Gas Chromatograph coupled to a Finnigan Mat 252 Isotope Ratio Mass Spectrometer. Porewater concentrations of dissolved organic acids were measured via HPLC (Albert and Martens, 1997).

2.6. Single filament SIMS measurements

Single white filaments of 120 μm diameter from the 1998 Guaymas cruise were prepared on silicon wafers and subjected to $\delta^{13}C$ analysis on a CAMECA-IMS6F Secondary Ion Mass Spectrometer (SIMS) located at the Analytical Instrumentation Facility of North Carolina State University. Filament isotope ratios were determined by also sputtering *Escherichia coli* cells that had also been measured by MS (Finnigan Mat 252 Isotope Ratio Mass Spectrometer) to determine instrumental mass fractionation. A total of three *E. coli* samples were used as controls and three individual filaments were measured.

3. Results and discussion

3.1. Molecular analyses

16S rRNA gene sequences from four orange and two white Guaymas *Beggiatoa* filaments were incorporated into a phylogenetic tree with 28 closely related species of the phylum Gammaproteobacteria (Fig. 1). According to the recently updated *Beggiatoa* phylogeny by Salman and colleagues (2011), our sequences fall into the *Maribeggiatoa* and *Parabeggiatoa*, groups of uncultured, marine, large, vacuolated, nitrate-accumulating, filamentous sulfur oxidizers. These groups have the indeterminate taxonomic status of *Candidatus*, used for incompletely described organisms that await further taxonomic identification (Murray and Stackebrandt, 1995). For the purposes of this study, we retain the term *Beggiatoa*, with the caveat that it designates phylogenetically divergent sulfur oxidizing filaments in Guaymas mats. The six sequences represent three separate 16S rRNA lineages, one for white forms of *Beggiatoa* and two for orange forms of *Beggiatoa*. 16S rRNA sequences from one orange filament collected on the 2008 cruise and another orange filament from 2009, both with diameters of ~24 μm, are 100% identical; however, they are only 99% and 95% similar to the two other orange *Beggiatoa* filaments collected in 1998 (35 μm filament diameter) and 2008 (diameter unknown, but less than 60 μm), respectively. The 16S rRNA sequences from the two white filaments collected in 1998 and 2009, both representing the 120 μm filament diameter size class (Nelson et al., 1989), are 99% identical with only six base pair mismatches. The 16S rRNA gene sequences of orange and white *Beggiatoa* from Guaymas Basin reveal species-level diversity between the orange and white filaments, as well as within the orange group alone, based on the 3% cutoff proposed by Stackebrandt and Goebel (1994). Neither color groups nor size classes alone are sufficient to describe the diversity of Guaymas *Beggiatoa*. From this analysis we propose that the change in color across a *Beggiatoa* mat is not a physiological variable within otherwise closely related or identical organisms, but marks phylogenetically distinct bacteria that generally prefer distinct microhabitats within the same mat.

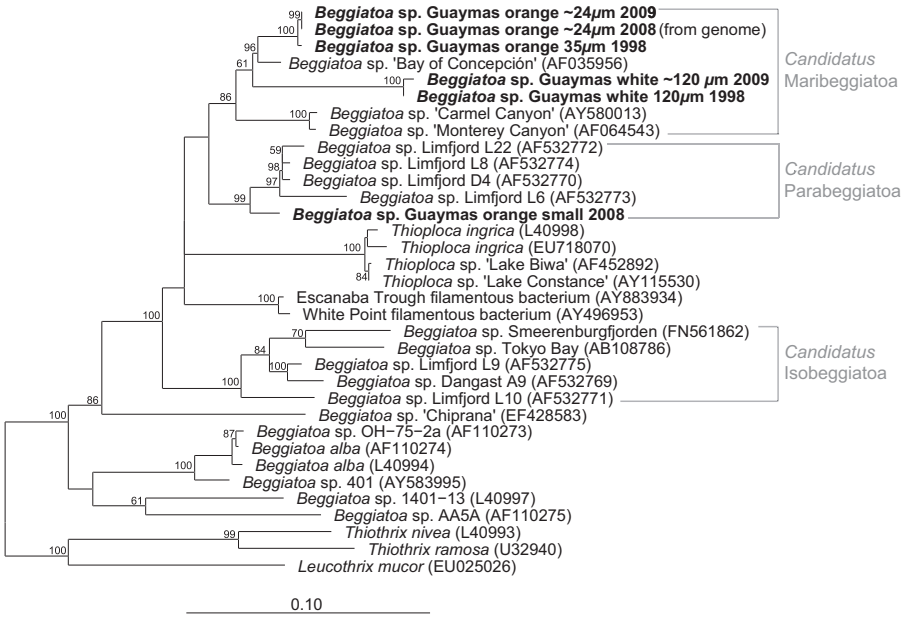

Fig. 1. Phylogenetic tree based on the gene sequence for the 16S small subunit ribosomal RNA from six *Beggiatoa* filaments isolated during our two cruises to Guaymas Basin in 2008 and 2009, and a previous cruise in 1998. Guaymas *Beggiatoa* sequences were aligned with sequences from 28 related filamentous bacteria within the Gammaproteobacteria. Diameters of the two *Beggiatoa* spp. from 1998 were measured in detail and are given, while diameters from the 2008 and 2009 specimens are approximations obtained by shipboard dissection microscopy. Estimated diameters correspond with width classes put forth by Nelson and colleagues (1989) for Guaymas *Beggiatoa* spp. One orange filament from 2008 is labeled "small", indicating that it falls within one of the two smaller width classes (24 or 42 μm). Recently suggested candidate groups (Salman et al., 2011) are indicated as brackets on the right.

3.2. Surface temperatures

To examine the general spatial relationship between *Beggiatoa* mat cover and active hydrothermal seepage, 14 temperature profiles were taken in and around a hydrothermally active site with extensive mat cover, termed MegaMat (Dive 4485, December 8, 2008, 27°N00.464, 111°W24.512). A 3-dimensional reconstruction of MegaMat temperature profiles exhibits a characteristic feature of *Beggiatoa* mats in hydrothermally active sediments: central portions of mats have hotter subsurface temperatures, which decrease considerably as temperature measurements approach bare sediments at the mat's edge (Fig. 2). In situ temperature readings for *Beggiatoa* mats at the surface of MegaMat do not exceed 16.5 °C, indicating that Guaymas *Beggiatoa* colonize the relatively cool sediment-water interface above hydrothermally active sediments, which reach temperatures up to 200 °C just 35 cm beneath MegaMat (profile 13). To check this trend with temperature data from other Guaymas Basin locations, surface and subsurface (40 cmbsf) temperatures from 78 temperature profiles taken at 15 different mat systems with both orange and white filaments were grouped by mat color, or by distance from the edge of a mat in the case of bare sediment profiles (Fig. 3). Group "O" consists of temperature profiles taken in orange portions of mats (which may have some white filaments), group "W" consists of profiles taken in white portions of mats in which no orange filaments were detected (by inspection of mat tufts with a dissection microscope), group "S" consists of profiles taken in nearby bare sediments (<1 m from a mat), and group "B" consists of profiles taken in background sediments (>1 m from a mat). A *post hoc* Tukey test comparing surface temperatures to subsurface temperatures within each group finds that depth influences temperature in groups O, W, and S (denoted by asterisks), but not in group B, which has relatively cool temperatures at every depth (Fig. 3). This observation is consistent with previous results that Guaymas Basin sediments without hydrothermal seepage have temperatures near the seawater background of 3 °C (Gundersen et al., 1992). Of the 78 temperature profiles obtained, 60 included an individual temperature reading exactly at the *Beggiatoa*-inhabited sediment-water interface. Surface temperatures in bare sediments near mats (group S) range from 3 to 7 °C while background surface temperatures (group B) remain low, near 3 °C. The Tukey test does not interpret any group as encompassing significantly warmer surface temperatures than any other group (denoted by *a* in Fig. 3). However, because all groups have a clearly defined lower limit surface temperature of 3 °C set by ambient seawater conditions, and a less consistent upper limit surface temperature determined by the hydrothermal activity beneath a given mat, surface temperature averages for all groups are weighted towards 3 °C. While surface temperatures within the two *Beggiatoa*-inhabited groups, O and W, range from 3 °C to occasionally as high as 60 °C, most surface temperature measurements are in the 3–16 °C range (Fig. 4). This cool surface temperature range indicates that Guaymas Basin *Beggiatoa* are not thermophilic, as might be assumed from their association with hydrothermal seepage, but live at relatively cool temperatures. The in situ temperatures of Guaymas Basin *Beggiatoa* mats are consistent with temperature optima near 20 °C for CO_2 assimilation by intact *Beggiatoa* filaments (Nelson et al., 1989), even over a wide range of habitat types (Dunker et al., 2010). This is also consistent with prior in situ temperature sensor measurements of 3–5 °C just 1 cm above *Beggiatoa* mats at Guaymas Basin (Gundersen et al., 1992).

The upper extent of the standard deviation from the mean of all surface temperatures from all mats is 21 °C, as plotted in Fig. 4. Closer examination of groups O and W reveals that orange *Beggiatoa* filaments were observed at in situ temperatures above 21 °C more often than white *Beggiatoa* filaments (6 observations vs. 2 observations). If the dataset of surface temperatures from *Beggiatoa* mats is expanded to include the 28 readings in mats with only white filaments (and no orange filaments) as well as orange and white mats, the upper extent of the standard deviation changes minimally, to 22 °C. High temperatures above this limit, or statistical outliers, are found in 23% of all measurements in orange sections ($n=26$), in contrast to either 5.9% in white sections adjacent to orange sections ($n=34$), or 8.1% in all white sections ($n=62$; not shown in Fig. 4), including those with no nearby orange sections. These surface temperature outliers could

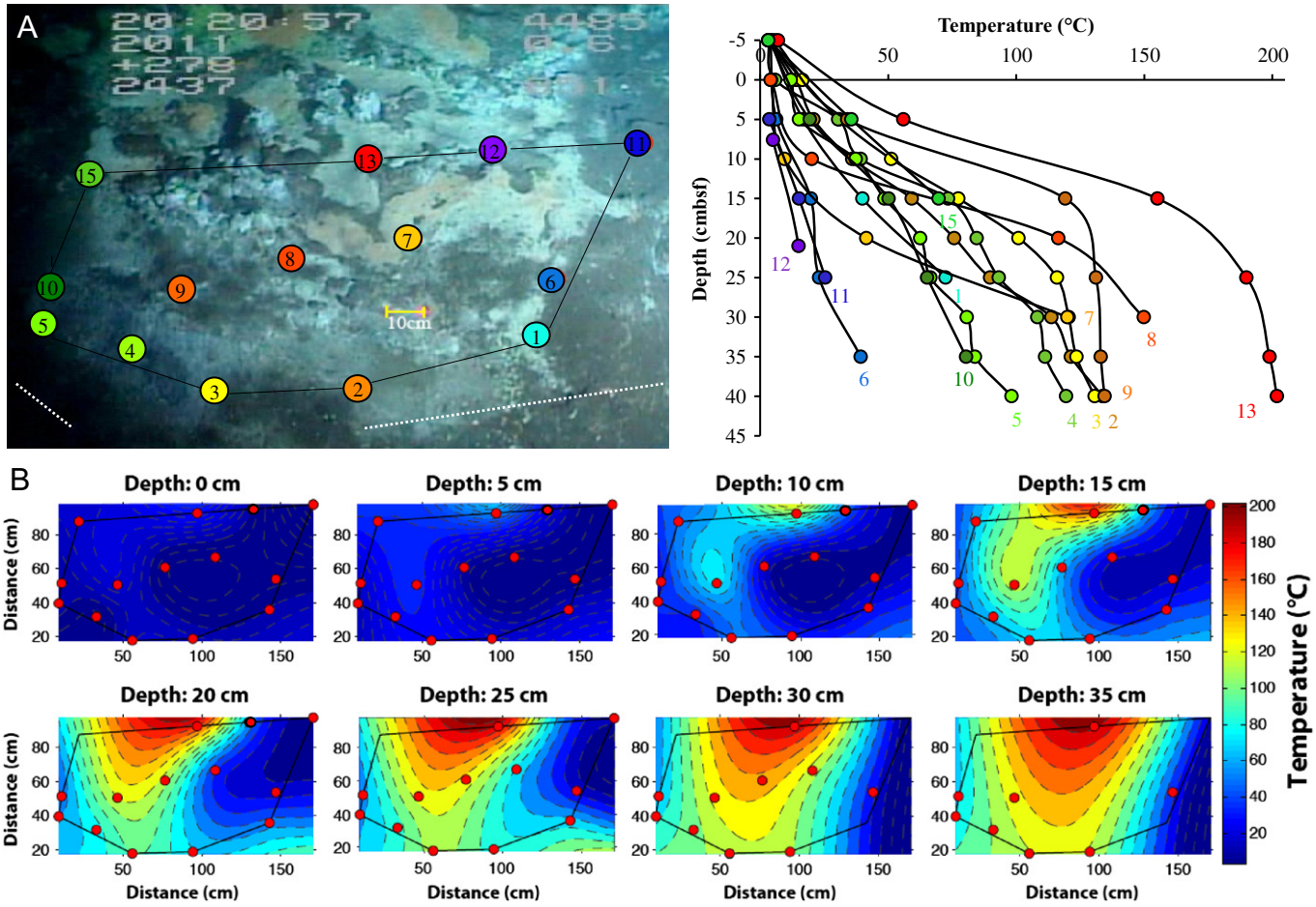

Fig. 2. (A) MegaMat hydrothermal area with 14 color-coded temperature measurement points and their corresponding temperature profiles. The black line marks the area of measured temperature data. A 10 cm scale bar is shown as the yellow line. (B) Contour plots of reconstruction of temperature field in 5 cm sediment depth intervals. Only temperature data within the measured depth interval were used for calculation of the reconstructed temperature field (red dots). Short temperature profiles were not extrapolated vertically, no red dots are plotted in such cases, and temperatures at these spots were inferred based on *x*/*y* interpolation from neighboring T data points only.

represent more frequent surges in hydrothermal flux beneath the predominantly orange center of a mat than the white periphery; as a corollary, orange *Beggiatoa* may have developed greater thermotolerance than white *Beggiatoa*. Enzyme activities support this interpretation. Narrow, pigmented *Beggiatoa* filaments at Guaymas Basin have peak enzymatic activities of D-ribulose-1, 5-bisphosphate carboxylase/oxygenase (RuBisCO) at thermophilic temperatures around 50 °C, while CO_2 incorporation rates peak at only 20 °C (Nelson et al., 1989); this observation is discussed as a possible adaptation to fluctuating hydrothermal temperatures (Nelson et al., 1989). However, we acknowledge the caveat that our data represent one-time snapshots of *Beggiatoa* communities that move and rearrange in response to a dynamic hydrothermal system, and we cannot be sure whether outliers represent temporary surges or sites where elevated hydrothermal flux is more persistent. Daily photo surveys of a *Beggiatoa* mat on our 2009 cruise demonstrated subtle but noticeable changes in surface texture over 11 days, which could indicate rapid fluctuations in subsurface hydrothermal flow. Moreover, a well-developed *Beggiatoa* mat with subsurface temperatures of 50 °C (Marker 6) was documented during our 2008 cruise, but had disappeared in 2009; only bare sediment with a subsurface temperature (at 40 cmbsf) of less than 6 °C was found at this site (Fig. S1).

3.3. Subsurface temperatures.

While surface temperatures illuminate in situ temperature ranges of Guaymas *Beggiatoa* spp., subsurface temperatures provide information related to the strength of hydrothermal flow beneath the mat. The average temperatures at 40 cmbsf from groups O and W are not significantly different from one another, but both are significantly warmer than average temperatures below bare sediments in groups S and B (denoted by $ and #, respectively, Fig. 3). These observations are consistent with our working hypothesis that hydrothermal activity and temperatures are higher beneath mat cover than beneath bare sediments, whether bare sediments are near or far from a mat. The average 40 cmbsf-temperatures for all 15 mats with zones of both orange and white *Beggiatoa* do not suggest a predictive relationship between filament color and subsurface temperature (Fig. 3), in the sense that a particular subsurface temperature should always correspond to a specific *Beggiatoa* color. Temperature regimes change considerably from one mat to the next, and temperature ranges beneath *Beggiatoa* of the same color but from different mats can be distinct from one another.

From dives 4490, 4569, and 4572, we measured in situ temperature profiles and porewater profiles of sulfide and sulfate concentrations, DIC concentration and $\delta^{13}C$ values, methane

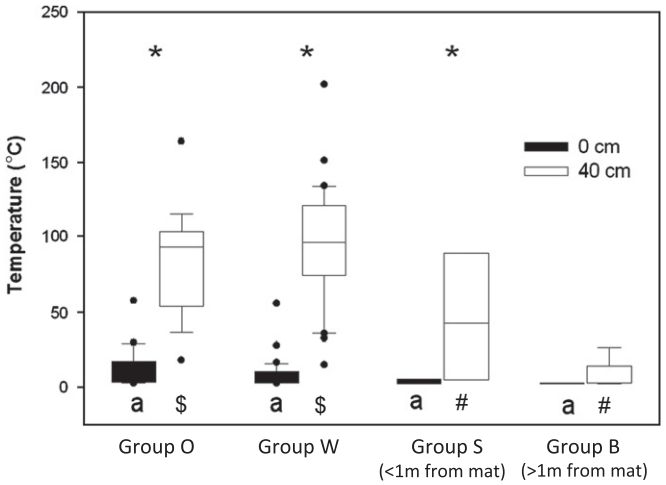

Fig. 3. Box and whisker plot depicting the in situ temperatures for the sediment-water interface (0 cm) and 40 cm sediment depth for orange (Group O) and white (Group W) *Beggiatoa* mats, sediments near the mats (Group S), and cold background sediments distant from microbial mats (Group B). The boxes encompass temperature points within the 25–75th percentile range. A line through a box represents the median temperature of the group at either 0 cm or 40 cm depth. The whiskers represent the 10th percentile (at the top) and the 90th percentile (at the bottom). Points outside of the whiskers are considered outliers. The asterisks denote groups in which temperature is influenced by depth with statistical support (*post hoc* Tukey test). No significant difference was found between surface temperature averages between any group; all averages fall into statistical bin *a*. Subsurface temperatures from groups O and W fall into statistical bin *$*, and are statistically different from subsurface temperatures of groups S and B, which fall into bin #. Sample sizes for each group and depth in the sediment: Group O – 26 (0 cm) and 19 (40 cm); Group W – 34 (0 cm) and 33 (40 cm); Group S – 7 (0 cm) and 6 (40 cm); Group B – 8 (0 cm) and 9 (40 cm). Average surface temperatures are 12.1 °C for Group O (st dev=12.7), 8.7 °C for Group W (st dev=10.0), 4.1 °C for Group S (st dev=1.7), and 3.2 °C for Group B (stdev=0.6). Average subsurface (40 cmbsf) temperatures are 86.0 °C for Group O (st dev=33.7), 96.3 °C for Group W (st dev=37.5), 46.2 °C for Group S (st dev=40.4), and 8.3 °C for Group S (st dev=9.6).

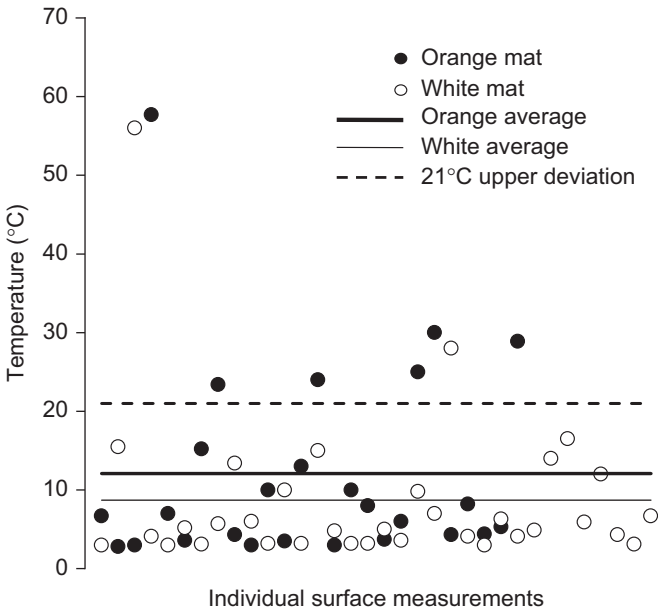

Fig. 4. Sixty individual temperature readings in orange and white *Beggiatoa* mats taken exactly at the sediment surface. The lines indicate the temperature average for orange (12.1 °C) and white *Beggiatoa* mats (8.7 °C). Although most data points are in the low temperature range (<10 °C), some high temperature measurements above the upper extent of standard deviation from the mean (21 °C, dashed line) are present, and are found more frequently in orange *Beggiatoa* mats than in white mats.

concentration and δ^{13}C-values, and short-chain organic acid concentrations. Temperature measurements and push cores for porewater analysis were taken in closely-spaced transects across three separate orange and white *Beggiatoa* mats, allowing unambiguous color groupings in close proximity for optimal comparison (Fig. 5). During dive 4483, temperatures were taken in a similar transect from orange to white to bare sediment, but no cores were taken and no geochemical data are available (Fig. S2, supplementary information). Mats from dives 4490, 4569, 4572, and 4483 will now be referred to as mats 1, 2, 3 (Fig. 5A–C), and 4 (supp. Fig. S2), respectively. All surface temperatures from mats 1, 2, and 4 are 3 °C except in the orange portion of mat 2, which at 13 °C remains within the expected range of surface temperatures in *Beggiatoa* mats (see above), while all subsurface temperatures increase with depth. Surface temperatures from mat 3 are not available, but subsurface temperatures also increase with depth. Profiles taken in bare sediments with no mat cover yield the coolest temperatures. Next to mats 1 and 4, the bare sediment profiles at 10 cm distance from mat cover were warmer than the bare-sediment temperature profiles next to mats 2 and 3, at 25 and 15 cm distance, respectively. As expected, elevated temperatures due to hydrothermal activity decrease with increasing distance from *Beggiatoa* mats.

Transects of temperature profiles for individual mats show that the typical sequence of orange and white *Beggiatoa* mats are supported by hydrothermal fluid of different temperatures (Figs. 5 and 6). Orange filaments in mats 1, 2 and 4 are positioned over the subsurface temperature maximum (at 40 cmbsf) and are surrounded by white mats overlying cooler sediments. At the same time, there are no predictive temperature regimes for orange versus white mats, since the temperature ranges associated with white or orange *Beggiatoa* can shift from one mat to another. For example, at 40 cm sediment depth, the temperature regimes below *Beggiatoa* filaments of the same color in mats 2 and 4 are 15–30 °C lower than in their mat 1 counterparts. Instead, temperature preferences appear to be relative within a given hydrothermally active sediment area. Mat 3 provides an interesting exception to the rule that orange *Beggiatoa* filaments congregate above the relative subsurface temperature maximum. Here, the temperature profile underneath white *Beggiatoa* is initially cooler than the orange mat-associated temperature profile, but it steepens downcore, and surpasses the temperature of the orange profile at a depth of 25 cmbsf. These temperature curves could result from lateral fluid flow, where the hottest fluid passes sideways or at an angle underneath the white mat before it approaches the sediment surface laterally offset underneath the orange mat.

If temperature provides an applicable proxy, hydrothermal fluid flow (and presumably supply of metabolic substrates to microorganisms) may be greater to the orange than the white portions of *Beggiatoa* mats. Although a definitive calculation of hydrothermal flux cannot be achieved from the current dataset, Fourier's law for the transfer of heat demonstrates the tendency of a heat flux, whether conductive, convective, or a combination of both, to (i) increase with the magnitude of a gradient and (ii) be in a direction opposite to the direction of the gradient. As such, higher temperature gradients imply higher heat fluxes. Because hydrothermal fluids are both a source of heat and of reduced organic and inorganic compounds to surface sediments, an increase in heat flux implies a related increase in delivery of electron donors and carbon sources to the *Beggiatoa* living at the sediment-water interface. Steeper temperature gradients exist beneath the orange portions of three out of four mats, and temperature profiles below bare sediments are lowest for all four mats. Thus, it appears

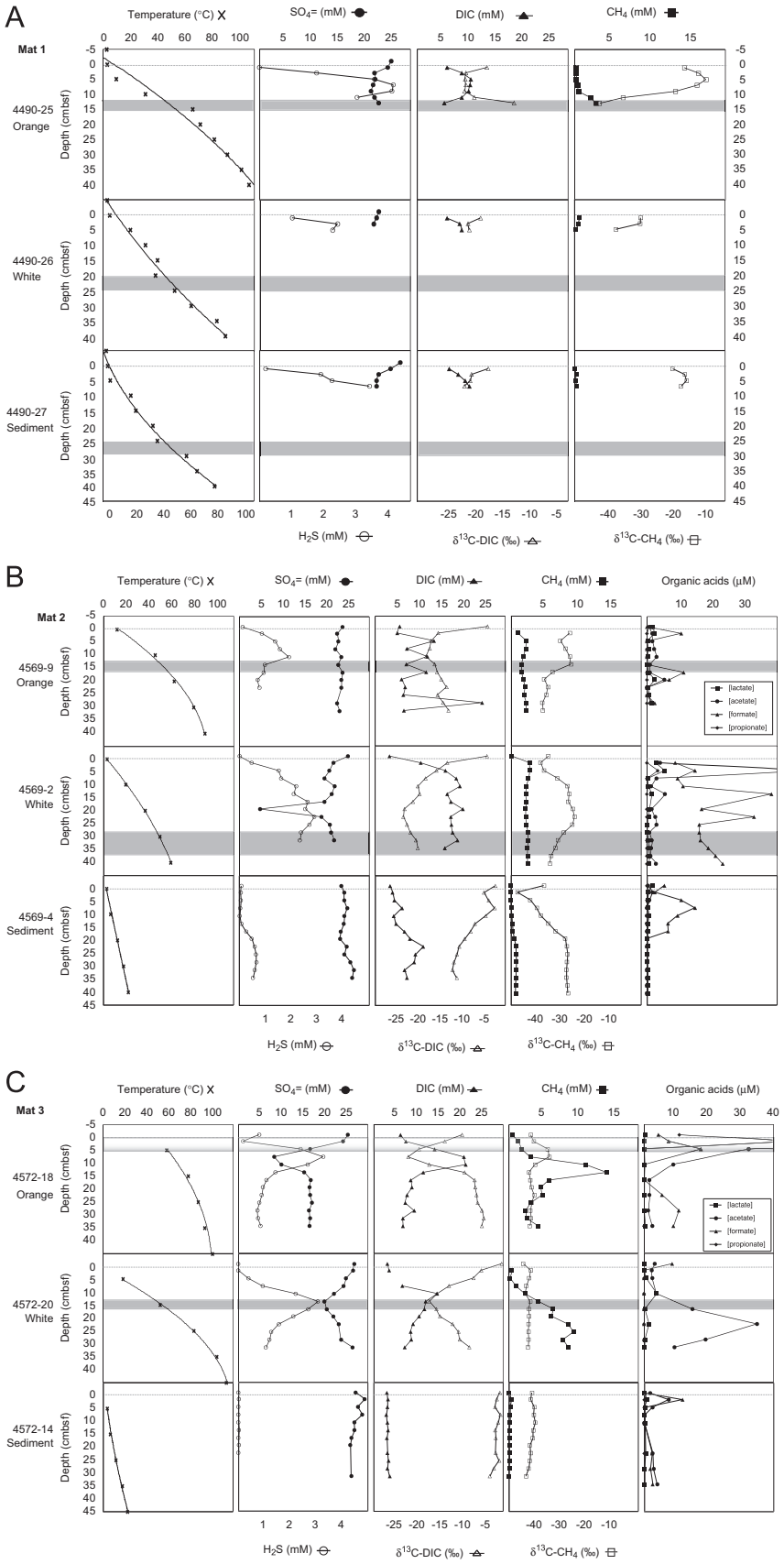

Fig. 5. Temperature, sulfide, sulfate, DIC concentration and isotope, and methane concentration and isotope profiles (for mats 1, 2, and 3), as well as organic acid profiles (for mats 2 and 3; expanded profiles shown in Fig. S3, supplemental information) for comparison of temperature and geochemical regimes along gradients from orange mat to white mat to nearby sediments. Gray shaded areas represent the 50–60 °C isotherms. (A) Mat 1. *Beggiatoa* mat ca. 25 m southwest of Megamat, Dive 4490, Dec 14, 2008 (27°N0.446, 111°W24.532). (B) Mat 2. *Beggiatoa* mat at Marker 14, Dive 4569, Nov. 30, 2009 (27°N0.47, 111°W24.431). (C) Mat 3. *Beggiatoa* mat at Marker 27, Dive 4572, Dec. 2, 2009 (27°N0.445, 111°W24.529). Several instances occurred in which organic acid concentrations exceeded the range of the plot: acetate concentrations reach 50.1 μM at 1.5 cmbsf in the white section of mat 2; acetate concentrations reach 73.8 μM in the overlying seawater and 295 μM at 1.5 cmbsf in the orange section of mat 3; propionate concentrations reach 46.0 μM at 1.5 cmbsf in the orange section of mat 3 (Fig. S3).

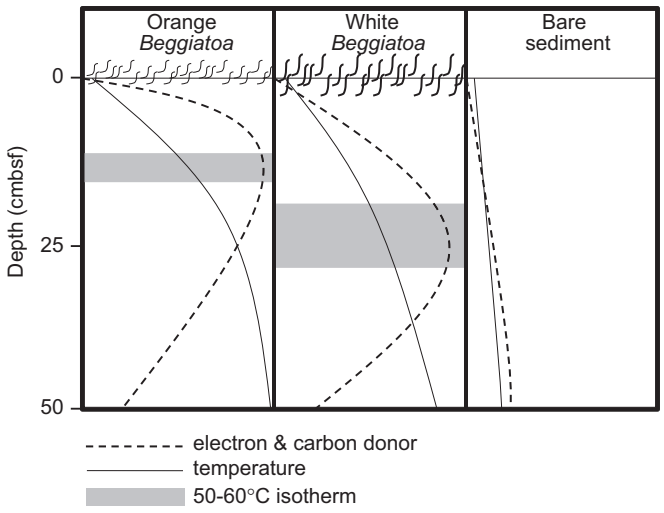

Fig. 6. Concept outline of subsurface thermal and geochemical gradients beneath orange and white *Beggiatoa* filaments within the same mat. Thin solid lines correspond to temperature profiles, thick dashed lines correspond to carbon source/electron donors, and gray boxes represent 50–60 °C isotherms. Depth in cmbsf is shown on the *y* axis. Temperature between 0 and 100 °C, as well as carbon source/electron donor concentrations in arbitrary units, are plotted on each *x* axis, increasing from left to right.

that within a given mat, orange *Beggiatoa* filaments usually concentrate over the local hydrothermal flux maximum and may therefore receive the greatest supply of carbon sources and metabolically relevant electron donors like sulfide. However, this interpretation might be too simplistic for two reasons. First, temperature and microbial substrate flux supporting mat growth may not always be proportionally linked; substantial variation may be caused by localized cooling of vent fluids by ambient seawater introduced from above, temporal changes in fluid flow, or subsurface microbial activity levels. Second, temperature and hydrothermal flux maxima could impact *Beggiatoa* mats indirectly by pushing subsurface anaerobic remineralization and respiration processes that produce sulfide, DIC or hydrothermally produced carbon substrates towards the surface sediments. These possibilities were investigated by measurements of sulfate, sulfide, DIC isotopes and concentrations, and CH_4 isotopes and concentrations in the shallow subsurface beneath mats 1, 2, and 3, as well as organic acid concentrations beneath mats 2 and 3.

3.4. Porewater geochemical profiles of individual mats

In mat 1, sampling constraints due to short coreliners limited the geochemical characterization (Fig. 5A), yet the orange *Beggiatoa* core documented characteristic porewater profiles indicative of sulfate reduction, methane oxidation, and DIC accumulation. An equimolar decrease in sulfate concentration and increase in sulfide concentration by ~4 mM occurs within the upper 15 cm beneath the orange *Beggiatoa*, indicative of biological sulfate reduction. The sulfide maximum/sulfate minimum zone coincides with a DIC peak and δ^{13}C-DIC isotope shift towards lighter values near −20‰, consistent with microbial remineralization of photosynthetic biomass. High CH_4 porewater concentrations above atmospheric saturation near the bottom of the core decrease towards the sediment surface, concomitant with increasingly heavy values of δ^{13}C-CH_4, from < -40‰ at depth (characteristic for Guaymas Basin; Welhan, 1988; Pearson et al., 2005) to near −10‰ at the sediment surface. This isotopic trend is indicative of biological methane oxidation; sulfate is available throughout the sediment column as an electron acceptor for methane oxidation (see also Suppl. Text). The in situ temperature regime reaches 50–60 °C near the bottom of the core, which is compatible with high-temperature-adapted, sulfate-dependent methane oxidation observed in enrichments (Holler et al., 2011), in situ geochemical profiles (Biddle et al., 2011) and thermophilic sulfate reduction (Jørgensen et al., 1990; Elsgaard et al., 1994; Weber and Jørgensen, 2002).

The white *Beggiatoa* core and nearby sediment core from mat 1 were very short, but the truncated porewater profiles were consistent with the tops of the orange *Beggiatoa* profiles and indicated similar processes at the shallowest depths. Since the closely spaced cores in mat 1 showed similar temperature profiles, coring sites in mats 2 and 3 were spaced further apart to sample distinct temperature gradients.

In mat 2, the porewater gradients change systematically from the center of the mat, dominated by orange *Beggiatoa* spp., to the peripheral mat of white *Beggiatoa* spp., to bare sediment (Fig. 5B). Along this gradient, the peaks of the broad porewater sulfide profiles shift towards deeper sediment layers, from near 10 cm underneath the orange mat, to ca. 20–25 cm underneath the white mat, to ca. 25–30 cm in the bare sediment, here with much reduced sulfide porewater concentrations. The orange and white mat cores show broad zones of DIC enrichment (complicated by strong downcore DIC fluctuations in the former core; unfortunately, replicate samples for consistency checks were not available) coinciding with light δ^{13}C-DIC values around −15‰ to −20‰ that reflect the impact of remineralization of buried photosynthetic biomass, and potentially contributions from other isotopically light DIC sources, such as methane oxidation. The lightest δ^{13}C-DIC values shift in congruence with the sulfide peaks, from ca. 10 cm underneath the orange mat, to 20–25 cm below the white mat, towards 30 cm in the bare sediment. In the bare sediment, lower DIC concentrations (< 10 mM) coincide with heavier δ^{13}C-DIC values (≥ -12‰), consistent with diminished remineralization of buried biomass. Porewater methane concentrations underneath the orange and white *Beggiatoa* mat are higher than in the nearby bare sediment; the δ^{13}C-CH_4 signatures show the impact of microbial methane oxidation underneath the orange and white mats, where δ^{13}C-CH_4 shifts from ca. −40‰ to −35‰ towards > -25‰, within the upper 20 cm of the sediment column (orange mat) or from 40 to 25 cm depth (white mat). Thus, sulfide concentration maxima, δ^{13}C-DIC minima, and δ^{13}C-CH_4 trends of methane oxidation are located closer to the sediment surface underneath the orange mat, move deeper into the sediment underneath the white mat, and shift deeper still or disappear entirely within the bare sediment. This trend is consistent with expanding temperature gradients from orange mat to white mat to bare sediment; for example, the 50 °C isotherm (compatible with anaerobic, sulfate-dependent methane oxidation and thermophilic sulfate reduction), moves from ca. 10 cm depth below the orange mat to ca. 25 cm depth below the white mat, and below coring range (50 cm) in the bare sediment.

As in mat 2, the sediment porewater gradients of mat 3 (Fig. 5C) change systematically from sediments beneath the orange *Beggiatoa* spp. in the center, to those covered by white *Beggiatoa* spp., to bare sediment. Sulfide maxima and matching sulfate minima shift from ca. 8 cm depth under the orange mat, to ca. 14 cm depth below the white mat, and are not detectable in the bare sediment. The orange and white mat cores show a distinct DIC concentration peak that coincides with light δ^{13}C-DIC values near −20‰, consistent with bioremineralization of buried photosynthetic biomass, and a potential smaller contribution of methane-derived DIC. As in mat 2, the δ^{13}C-DIC minima shift downcore in parallel with the sulfide maxima and sulfate minima: from ca. 8 cm depth underneath the orange mat to ca. 14 cm below the white mat. Under the orange mat, very high

methane concentrations of 15 mM near 14 cm depth decrease towards the sediment surface; this trend coincides with heavier $\delta^{13}C$-CH_4 values (from ca. 14 to 8 cm depth) indicative of methane oxidation. Similar drops in methane porewater concentrations appear shifted downcore under the white mat, at ca. 25 cm depth. Thus, sulfide concentration maxima and sulfate concentration minima, methane concentration maxima, and negative $\delta^{13}C$ signatures of bioremineralization to DIC are located closer to the sediment surface underneath the orange mat, move deeper into the sediment underneath the white mat, and disappear or decrease substantially in the bare sediment outside the mat. Here, sulfide and methane do not accumulate within the cored sediment depth, and DIC concentrations remain constant near 3–4 mM. As in mat 2, this trend is congruent with the changing temperature gradients from orange mat to white mat to bare sediment. For example, moving from orange to white, the 50 °C isotherm moves from <5 to 15 cm depth, and the 60 °C isotherm (both compatible with anaerobic, sulfate-dependent methane oxidation and thermophilic sulfate reduction) moves from 5 cm depth below the orange mat to ca. 15–20 cm depth below the white mat, and below coring depth (50 cm) in the bare sediment. Although the white mat profile reaches higher temperatures at depth than the orange mat profile, the white profile starts cooler near the sediment surface and does not surpass the orange profile until temperatures are ca. 85 °C, well above the previously mentioned 50–60 °C range.

These patterns suggest that the in situ temperature gradients of hydrothermal sediments are one of the most important controls on microbial processes in the sediment. Shallow 50–60 °C isotherms beneath orange *Beggiatoa* mats shift the microbially active sediment layers, i.e., sediment horizons of sulfide accumulation due to sulfate reduction, increased DIC concentrations, and isotopic indicators of bioremineralization and methane oxidation, closer to the sediment surface. In contrast, the 50–60 °C isotherms reach deeper beneath adjacent white *Beggiatoa* mats, permitting downcore extension of sedimentary microbial processes (shaded in gray, Fig. 5A–C). We note that porewater concentrations are not a substitute for process rates, or a basis for inferring rates, given the likelihood of advective transport and non-steady state conditions in Guaymas surface sediments (Gundersen et al., 1992). The porewater gradients documented here are therefore most realistically viewed as the result of a complex interplay of in situ microbial process rates (sulfate reduction, sulfide reoxidation, methanogenesis, methane oxidation, other terminal oxidation processes that increase the DIC pool), upward and lateral advection of hydrothermal flow, downward and lateral seawater inmixing, and the diffusive properties of the sediments.

The contrast between the geochemical gradients in the bare sediment and mat-covered sediment demonstrates the habitat requirements of Guaymas *Beggiatoa* spp.: the orange and white *Beggiatoa* mats require high sulfide concentrations – and thus steep sulfide gradients – near the sediment surface; the gradients show sulfide porewater concentrations of approximately 2–3 mM within the upper 5–10 cm. Porewater DIC in high concentrations (10–20 mM) in the same depth range, and methane in variable, often supersaturated concentrations also characterize the *Beggiatoa*-covered sediments. Parsimoniously interpreted, these steep gradients of sulfide and DIC are consistent with rapid sulfide and DIC flux to the sediment surface, and towards the *Beggiatoa* mat. The more subtle differences in habitat preference of orange versus white *Beggiatoa* spp. appear to be linked, directly or indirectly, to the temperature-controlled compression of subsurface microbial activity towards the sediment surface occupied by orange *Beggiatoa* spp. In contrast, more gradual porewater gradients and metabolic zones extend deeper into sediments underneath white *Beggiatoa* mats (Fig. 6).

3.5. Trophic mechanisms

We note that this interpretation assumes the white and orange Guaymas *Beggiatoa* spp. are autotrophic, and depend on fluxes of sulfide and DIC towards the sediment surface. However, assimilation and oxidation of organic compounds by the *Beggiatoa* mats cannot be ruled out; the conspicuous peaks of porewater acetate in surficial sediments under some mats (Fig. 5B and C) allow for the possibility that *Beggiatoa* spp. assimilate and oxidize this organic carbon source. Since some *Beggiatoa* strains have the ability to respire acetate (summarized in Larkin and Strohl, 1983), different physiological modes should be considered for Guaymas *Beggiatoa* spp. Facultative autotrophy has been suggested as a possible physiological mechanism of *Beggiatoa* spp. in both hydrothermal vent sites (Nelson et al., 1989) and at cold seeps (Nikolaus et al., 2003). Our SIMS analysis of individual 120 μm white filaments from Guaymas finds that individual filaments have a $\delta^{13}C$ averaging $-42‰$ (st dev=23). Despite this high deviation from the mean, comparison with other isotopic studies of Guaymas Basin microbial biomass and carbon sources (Pearson et al., 2005) suggests that these large white filaments assimilate carbon compounds that are ultimately derived from methane carbon.

In several investigations of cold hydrocarbon seeps in the Gulf of Mexico, colorful *Beggiatoa* mats showed a Guaymas-like spatial distribution of orange mats with white peripheries (Wirsen et al., 1992; Sassen et al., 1994; Larkin and Henk, 1996; Nikolaus et al., 2003). Hydrocarbon analysis of sediments under *Beggiatoa* mats revealed that, in comparison to white *Beggiatoa*, adjacent orange *Beggiatoa* reside over sediments with elevated concentrations of unresolved petroleum hydrocarbons, and 1 to 3 orders of magnitude higher methane and ethane concentrations (Sassen et al., 1994). White filaments from the same cold seep environments appear to be more active in CO_2 fixation while orange *Beggiatoa* filaments have a reduced capacity for assimilation of inorganic carbon (Wirsen et al., 1992; Nikolaus et al., 2003). Both of these observations lend themselves to the notion that at cold seep environments pigmented *Beggiatoa* tend to be more heterotrophic while non-pigmented *Beggiatoa* appear to be more autotrophic. By contrast, at hydrothermally active sites in Guaymas Basin, Nelson and colleagues showed strong RuBisCO activity – at similar levels to known lithoautotrophs – and CO_2 incorporation by narrow, pigmented *Beggiatoa* as well as wide, nonpigmented filaments (Nelson et al., 1989; personal communication with Douglas C. Nelson). Autotrophy may be a preferred or more widely distributed trait of *Beggiatoa* spp. at hydrothermal vents.

3.6. Storage capacity

Supposing our interpretation of this system is accurate and flux of energy sources is greatest to the predominantly orange center of the mat, the distribution of orange and white *Beggiatoa* in a mat could be explained in terms of storage capacity. Orange *Beggiatoa* filaments have a smaller diameter and fall into the two smaller width classes of ~25 and ~35 μm, whereas white filaments fall into the largest width class of ~120 μm (Nelson et al., 1989). The volume of the thin cytoplasmic layer where elemental sulfur can be stored is therefore most likely smaller in orange *Beggiatoa* than in white *Beggiatoa*, although the difference remains to be constrained more accurately. Thus, the orange *Beggiatoa* filaments have a smaller capacity than white filaments for storage of electron donor in the form of elemental sulfur within their cytoplasm, and therefore cannot persist as long as white filaments during periods of inadequate delivery of energy sources. This could also explain why white filaments are found

throughout the mats while orange filaments appear restricted to the center, as white filaments may have the ability to grow further from the direct hydrothermal source. Although an increase in filament diameter – and thus in electron donor storage space – might imply the need to support a greater biomass, McHatton and coworkers observed decreasing protein-to-biovolume ratios with increasing *Beggiatoa* filament widths (McHatton et al.,1996), suggesting proportionally less biomass for larger filaments. Further studies to assess the thickness of the periplasmic layer, such as freeze-fracture and transmission electron microscopy (Strohl et al., 1982; Costello 2006; Larkin and Henk 1996), or direct concentration measurements of elemental sulfur stored within filaments (Zopfi et al., 2001), are needed to determine the capacity of a *Beggiatoa* filament to store electron donors.

4. Conclusion

The presently uncultivated orange and white *Beggiatoa* forms at Guaymas Basin represent separate phylotypes and species, and colonize the surface of hydrothermal sediments in contact with seawater at about 3 °C. Temperatures at the *Beggiatoa*-inhabited sediment-water interface usually range between 3 and 16 °C but can reach as much as 60 °C, while surface temperatures of non-*Beggiatoa* inhabited sediments are typically nearer ambient seawater temperatures of 3–4 °C. Because in situ temperature outliers were observed more frequently in orange mat areas than in white mat areas (Fig. 4), we suggest that orange filaments may be more thermotolerant than white filaments, but further studies are necessary to confirm this. Within a given mat, orange *Beggiatoa* spp. prefer surface sediments where high temperatures near the sediment surface (shallow 50–60 °C isotherms) lead to more compressed profiles of carbon and energy sources (Fig. 6). We conclude that close proximity to high concentrations of electron donors and carbon sources in the microbially active shallow subsurface, and the resulting steep gradients and fluxes of these electron donors and carbon sources to the sediment surface, rather than the in situ temperature range by itself, controls the relative differential positioning of orange and white filaments within a *Beggiatoa* mat. Given the wide spectrum of different temperature and hydrothermal flux regimes between different mats, this orange/white pattern represents a relative preference or even a competitive balance among different *Beggiatoa* types that establishes itself within the constraints of different hydrothermal hot spots.

Future work will integrate functional-gene sequencing of orange and white *Beggiatoa* filaments and in situ temperature logger data that document temperature fluctuations and *Beggiatoa* mat response over several days.

Acknowledgments

This study was supported by NSF (Bio-Oce 0647633). We thank the R/V *Atlantis* and HOV *Alvin* crews for exemplary work and unflagging support during our dives in Guaymas Basin. HPM was in part supported by the Gulf of Mexico Gas Hydrate Consortium. JFB was supported by a NASA NPP fellowship administered by ORAU. We thank all shipboard scientists, especially Stefanie Grünke for compiling the latitudes and longitudes of our principal dive targets during our 2008 Guaymas expedition. We thank Fred Stevie at NCSU for the SIMS analysis of single white filaments. We are also very grateful for helpful insights from Andrea Anton, Brian White, Hans Røy, Patrick Gibson, and Zena Cardman, and for constructive comments and suggestions from two anonymous reviewers.

Appendix A. Supporting information

Supplementary data associated with this article can be found in the online version at http://dx.doi.org/10.1016/j.dsr.2012.04.011.

References

Albert, D.B., Martens, C.S., 1997. Determination of low molecular weight organic acid con-centrations in seawater and pore-water samples via HPLC. Mar. Chem. 56, 27–37.

Biddle J.F., Cardman Z., Mendlovitz H.P., Albert D.B., Lloyd K.G., Boetius A., and Teske A. (2011) Anaerobic oxidation of methane at different temperature regimes in Guaymas Basin hydrothermal sediments. ISME J., doi:10.1038/ismej.2011.164.

Cline, J.D., 1969. Spectrophotometric determination of hydrogen sulfide in natural waters. Limnol. Oceanogr. 14, 454–458.

Costello, M.J., 2006. Cryo-electron microscopy of biological samples. Ultrastruct. Pathol. 30, 361–371.

Dhillon, A., Teske, A., Dillon, J., Stahl, D.A., Sogin, M.L., 2003. Molecular characterization of sulfate-reducing bacteria in the Guaymas Basin. Appl. Environ. Microbiol. 69, 2765–2772.

Dhillon, A., Lever, M., Lloyd, K.G., Albert, D.B., Sogin, M.L., Teske, A., 2005. Methanogen diversity evidenced by molecular characterization of methyl coenzyme M reductase (*mcrA*) genes in hydrothermal sediments of the Guaymas Basin. Appl. Environ. Microbiol. 71, 4592–4601.

Dunker, R., Røy, H., Jørgensen, B.B., 2010. Temperature regulation of gliding motility in filamentous sulfur bacteria, *Beggiatoa* spp. FEMS Microbiol. Ecol. *73*, 234–242.

Edmond, J.M., Von Damm, K., 1985. Chemistry of ridge crest hot springs. Biol. Soc. Washington Bull. 6, 43–47.

Einsele, G., Gieskes, J.M., Curray, J., Moore, D.M., Aguayo, E., Aubry, M.P., Fornari, D., Guerrero, J., Kastner, M., Kelts, K., Lyle, M., Matoba, Y., Molina-Cruz, A., Niemitz, J., Rueda, J., Saunders, A., Schrader, H., Simoneit, B., Vacquier, V., 1980. Intrusion of basaltic sills into highly porous sediments, and resulting hydrothermal activity. Nature 283, 441–445.

Elsgaard, L., Isaksen, M.F., Jørgensen, B.B., Alayse, A.M., Jannasch, H.W., 1994. Microbial sulfate reduction in deep-sea sediments at the Guaymas Basin hydrothermal vent area: influence of temperature and substrates. Geochim. Cosmochim. Acta 58, 3335–3343.

Gundersen, J.K., Jørgensen, B.B., Larsen, E., Jannasch, H.W., 1992. Mats of giant sulphur bacteria on deep-sea sediments due to fluctuating hydrothermal flow. Nature 360, 454–456.

Holler, T., Widdel, F., Knittel, K., Amann, R., Kellermann, M., Hinrichs, K.-U., Teske, A., Boetius, A., Wegener, G., 2011. Thermophilic anaerobic oxidation of methane by marine microbial consortia. ISME J. 5, 1946–1956.

Jannasch, H.W., Nelson, D.C., Wirsen, C.O., 1989. Massive natural occurrence of unusually large bacteria (*Beggiatoa* sp.) at a hydrothermal deep-sea vent site. Nature 342, 834–836.

Jørgensen, B.B., Zawacki, L.X., Jannasch, H.W., 1990. Thermophilic bacterial sulfate reduction in deep-sea sediments at the Guaymas Basin hydrothermal vents (Gulf of California). Deep Sea Res. Part I 37, 695–710.

Kalanetra, K.M., Huston, S.L., Nelson, D.C., 2004. Novel, attached, sulfur-oxidizing bacteria at shallow hydrothermal vents possess vacuoles not involved in respiratory nitrate accumulation. Appl. Environ. Microbiol. 70, 7487–7496.

Larkin, J.M., Henk, M.C., 1996. Filamentous sulfide-oxidizing bacteria at hydrocarbon seeps of the Gulf of Mexico. Microsc. Res. Tech. 33, 23–31.

Larkin, J.M., Strohl, W.R., 1983. *Beggiatoa*, *Thiotrix*, and *Thioploca*. Annu. Rev. Microbiol. 37, 341–367.

Lloyd, K.G., Albert, D.B., Biddle, J.F., Chanton, J.P., Pizarro, O., Teske, A., 2010. Spatial structure and activity of sedimentary microbial communities underlying a *Beggiatoa* spp. Mat in a Gulf of Mexico hydrocarbon seep. PLoS One 5, e8738.

Ludwig, W., Strunk, O., Westram, R., Richter, L., Meier, H., et al., 2004. ARB: a software environment for sequence data. Nucleic Acids Res. 32, 1363–1371.

MacGregor B.J., Biddle J.G., Siebert J.R., Staunton E., Harbort C., Hegg E.L., Matthysse A.G., Teske A. (2012) Why are Orange Guaymas *Beggiatoa* Orange? ASLO Ocean Sciences Meeting, Salt Lake City, Utah, February 19–24, 2012.

Martens, C.S., Albert, D.B., Alperin, M.J., 1999. Stable isotope tracing of anaerobic methane oxidation in the gassy sediments of Eckernförde Bay, German Baltic Sea. Am. J. Sci. 299, 589–610.

McHatton, S.C., Barry, J.P., Jannasch, H.W., Nelson, D.C., 1996. High nitrate concentrations in vacuolate, autotrophic marine *Beggiatoa*. Appl. Environ. Microbiol. 62, 954–958.

Murray, R.G.E., Stackebrandt, E., 1995. Taxonomic note: implementation of the provisional status candidatus for incompletely described procaryotes. Int. J. Syst. Bacteriol. 45, 186–187.

Nelson, D.C., Wirsen, C.O., Jannasch, H.W., 1989. Characterization of large, autotrophic *Beggiatoa* spp. abundant at hydrothermal vents of the Guaymas Basin. Appl. Environ. Microbiol. 55, 2909–2917.

Nikolaus, R., Ammerman, J.W., MacDonald, I.R., 2003. Distinct pigmentation and trophic modes in *Beggiatoa* from hydrocarbon seeps in the Gulf of Mexico. Aquat. Microb. Ecol. 32, 85–93.

Pearson, A., Seewald, J.S., Eglinton, T.I., 2005. Bacterial incorporation of relict carbon in the hydrothermal environment of Guaymas Basin. Geochim. Cosmochim. Acta 69, 5477–5486.

Prince, R.C., Stokley, K.E., Haith, C.E., Jannasch, H.W., 1988. The cytochromes of a marine *Beggiatoa*. Arch. Microbiol. 150, 193–196.

Pruesse, E., Quast, C., Knittel, K., Fuchs, B., Ludwig, W., Peplies, J., Glöckner, F.O., 2007. SILVA: a comprehensive online resource for quality checked and aligned ribosomal RNA sequence data compatible with ARB. Nucleic Acids Res. 35, 7188–7196.

Salman, V., Amann, R., Girnth, A.C., Polerecky, L., Bailey, J.V., Høgslund, S., Jessen, G., Pantoja, S., Schulz-Vogt, H.N., 2011. A single-cell sequencing approach to the classification of large, vacuolated sulfur bacteria. Syst. Appl. Microbiol. 34, 243–259.

Sassen, R., MacDonald, I.R., Requejo, A.G., Guinasso, N.L., Kennicutt II, M.C., Sweet, S.T., Brooks, J.M., 1994. Organic geochemistry of sediments from chemosynthetic communities, Gulf of Mexico slope. Geo-Mar. Lett. 14, 110–119.

Schulz, H.N., Jørgensen, B.B., 2001. Big bacteria. Annu. Rev. Microbiol. 55, 105–137.

Strohl, W.R., Howard, K.S., Larkin, J.M., 1982. Ultrastructure of *Beggiatoa alba* strain B15LD. J. Gen. Microbiol. 128, 73–84.

Stackebrandt, E., Goebel, B.M., 1994. A place for DNA/DNA reassociation and 16S rRNA sequence analysis in the present species definition in bacteriology. Int. J. Syst. Bacteriol. 44, 846–849.

Teske, A., Sogin, M.L., Nielsen, L.P., Jannasch, H.W., 1999. Phylogenetic position of a large marine *Beggiatoa*. Syst. Appl. Microbiol. 22, 39–44.

Teske, A., Hinrichs, K., Edgcomb, V., Gomez, A., Kysela, D., Sylva, S.P., Sogin, M.L., Jannasch, H.W., 2002. Microbial diversity of hydrothermal sediments in the Guaymas Basin: evidence for anaerobic methanotrophic communities. Appl. Environ. Microbiol. 68, 1994–2007.

Teske, A., Edgcomb, V., Rivers, A.R., Thompson, J.R., Gomez, A., Molyneaux, S.J., Wirsen, C.O., 2009. A molecular and physiological survey of a diverse collection of hydrothermal vent Thermococcus and Pyrococcus isolates. Extremophiles 13, 905–915.

Van Damm, K.L., Edmond, J.M., Measures, C.I., Grant, B., 1985. Chemistry of submarine hydrothermal solutions at Guaymas Basin, Gulf of California. Geochim. Cosmochim. Acta 49, 2221–2237.

Weber, A., Jørgensen, B.B., 2002. Bacterial sulfate reduction in hydrothermal sediments of the Guaymas Basin, Gulf of California, Mexico. Deep Sea Res. Part I 49, 827–841.

Welhan, J.A., 1988. Origins of methane in hydrothermal systems. Chem. Geol. 71, 183–198.

Wirsen C.O., Jannasch H.W., Molyneaux S.J. (1992) Non-Symbiotic Microbiota as Associated with Chemosynthetic Communities. 6.1–6.13 From: MacDonald IR (editor) Chemosynthetic Ecosystems Study. Volume II: Technical report. Prepared by Geochemical and Environmental Research Group. U.S. Dept. of the Interior, Minerals Mgmt. Service, Gulf of Mexico OCS Regional Office, New Orleans, LA. 238 pp.

Zopfi, J., Kjær, T., Nielsen, L.P., Jørgensen, B.B., 2001. Ecology of *Thioploca* spp.: nitrate and sulfur storage in relation to chemical microgradients and influence of *Thioploca* spp. on the sedimentary nitrogen cycle. Appl. Environ. Microbiol. 67, 5530–5537.